Controllable Decomposition of $Ca(BH_4)_2$ for Reversible Hydrogen Storage

Y. Yan,*[a,b] D. Rentsch[b] and A. Remhof[b]

$Ca(BH_4)_2$ could reversibly store 9.6 wt% hydrogen based on the overall reaction of $Ca(BH_4)_2 \rightarrow 1/3CaB_6 + 2/3CaH_2 + 10/3H_2$. Formation of CaB_6 instead of elemental boron and/or high boranes (e.g. $CaB_{12}H_{12}$) in the dehydrogenation process is crucial for the rehydrogenation. Here, we reported two experimental protocols regarding how to form CaB_6 from the decomposition of $Ca(BH_4)_2$: (1) decomposition below melting point, e.g. 350 °C *via* CaB_2H_6 to CaB_6 and (2) decomposition above melting point, e.g. 400 °C *via* elemental boron to CaB_6.

Introduction

Hydrogen produced from renewable energies such as wind or solar is considered as an ideal and clean synthetic energy carrier that could replace the fossil fuels used today. The use of hydrogen as a fuel strongly relies on its safe and efficient storage and transport, particularly for mobile applications.[1, 2] Due to their combined high gravimetric and volumetric hydrogen densities associated with favorable thermodynamics, alkaline earth borohydrides are considered as ideal candidates for solid-state hydrogen storage.[3, 4] For example, calcium borohydride, $Ca(BH_4)_2$, displays an enthalpy change of of 36 ± 4 kJ/mol H_2 in the dehydrogenation reaction into CaB_6 according to Eq. 1.[5-7], which lies within the targeted window of 20-45 kJ/mol H_2 for reversible on-board storage.

$$Ca(BH_4)_2 \rightarrow 1/3CaB_6 + 2/3CaH_2 + 10/3H_2 \quad (\Delta H = 36 \pm 4 \text{ kJ/mol } H_2) \quad (1)$$

However, the decomposition of $Ca(BH_4)_2$ to CaB_6 is far more complex and involves multiple steps. Great efforts have been made to unveil its decomposition routes and improve the hydrogen sorption properties.[6-21] CaH_2 is commonly accepted as one of the final decomposition products. Several boron-containing compounds have been reported in the solid residue, including CaB_2H_x (Eq. 2),[8, 9] $CaB_{12}H_{12}$ (Eq. 3),[10-12] CaB_6 (Eq. 1),[6, 9, 11, 13, 15] and elemental boron (Eq. 4).[12, 14] CaB_2H_x is a crystalline intermediate observed by X-ray diffraction [8, 9] and we recently identified this species by ^{11}B NMR, where x is most likely to be 6.[20] It further decomposes into CaB_6 which enables the rehydrogenation, while $CaB_{12}H_{12}$ and elemental boron are considered as major obstacles for the reversibility.

$$Ca(BH_4)_2 \rightarrow CaB_2H_6 + H_2 \quad (2)$$

$$Ca(BH_4)_2 \rightarrow 1/6CaB_{12}H_{12} + 5/6CaH_2 + H_2 \quad (\Delta H = 35 \pm 1 \text{ kJ/mol } H_2) \quad (3)$$

$$Ca(BH_4)_2 \rightarrow B + CaH_2 + H_2 \quad (\Delta H = 57 \pm 3 \text{ kJ/mol } H_2) \quad (4)$$

So far there is no effective experimental protocol to avoid the formation of $CaB_{12}H_{12}$ and/or elemental boron and to form CaB_6 as the only boron containing decomposition product, i.e. to suppress decomposition as shown in Eq. 3 and Eq. 4.

In the past, parameters such as applied hydrogen pressure and temperature were used to select favorable reaction routes.[14] For example, hydrogen pressure has been successively applied in $LiBH_4$-based reactive hydride composites,[22-24] where the self-decomposition of $LiBH_4$ into $Li_2B_{12}H_{12}$ was suppressed and the formation of metal borides. In the case of $Ca(BH_4)_2$, hydrogen backpressures up to 20 bar were not able to suppress the formation of elemental boron, although it influenced greatly the decomposition routes.[14] We observed that temperature plays an important role in the decomposition reaction of $Ca(BH_4)_2$.[18] Decomposition below the melting point (T_m of ca. 370 °C), facilitates the formation of CaB_6. However, the effect of temperature on the decomposition reaction has not been fully understood. In the present study, we investigated the decomposition process of $Ca(BH_4)_2$ at 350 °C and 400 °C, i.e. above and below the melting point, respectively. We discussed the mechanism of the temperature dependent hydrogen release and proposed procedures to omit the reaction paths to the undesired decomposition products.

Experimental

The samples of $Ca(BH_4)_2$ (purity, 95%), amorphous boron and CaB_6 (purity, 95%) were purchased from Sigma-Aldrich and used as received. The H_2 desorption of $Ca(BH_4)_2$ was performed using a custom made pressure-composition-temperature (*pcT*) apparatus under dynamic vacuum (< 10^{-4} mbar). The samples were heated to the target temperatures with a ramp of 10 °C/min. After H_2 desorption, the samples were quenched to room temperature for further characterization by nuclear magnetic resonance (NMR) spectroscopy, Raman spectroscopy and by X-ray diffraction (XRD).

[a] *Interdisciplinary Nanoscience Center (iNANO), Aarhus University, DK-8000 Aarhus C, Denmark. yigang.yan@inano.au.dk*
[b] *EMPA, Swiss Federal Laboratories for Materials Science and Technology, CH-8600 Dübendorf, Switzerland.*

Solid state ^{11}B magic angle spinning (MAS) NMR experiments were performed on a Bruker Avance-400 NMR spectrometer using a 4 mm CP-MAS probe. The ^{11}B NMR spectra were recorded at 128.4 MHz at 12 kHz sample rotation applying a Hahn echo pulse sequence to suppress the broad background resonance of boron nitride in the probe. Pulse lengths of 1.5 μs (π/12 pulse) and 3.0 μs were applied for the excitation and echo pulses, respectively. For selected samples, ^{1}H-^{11}B cross polarization magic angle spinning (CP-MAS) NMR spectra were recorded using weak radio-frequency powers for spin locking of the ^{11}B nucleus on resonance. NMR experiments of D_2O solutions were carried out using a 5 mm inverse broadband probe at 25 °C. ^{11}B NMR chemical shifts are reported in parts per million (ppm) externally referenced to a 1M $B(OH)_3$ aqueous solution at 19.6 ppm.

XRD measurements were performed using a Bruker D8 diffractometer equipped with a Goebel mirror selecting Cu Kα radiation (λ = 1.5418 Å) and a linear detector system (Vantec). Samples for XRD measurements were filled and sealed under argon atmosphere into glass capillaries (diameter 0.7 mm; wall thickness 0.01 mm).

Raman spectra were obtained at room temperature on a Bruker Senterra instrument of 5 cm^{-1} spectral resolution (spatial resolution ≈ 5 μm) using a 532 nm laser.

All sample handling was carried out in in a glove box (MBraun), filled with purified Argon (pH_2O and pO_2 < 1 ppm) or under hydrogen pressure as specified.

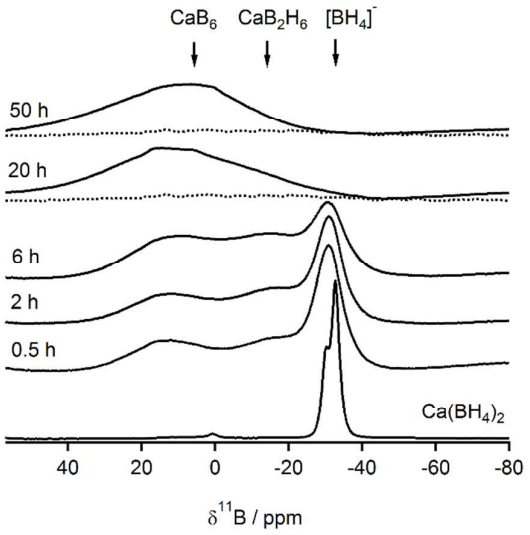

Fig. 1 ^{11}B MAS NMR spectra of $Ca(BH_4)_2$ dehydrogenated at 350 °C under vacuum for 0.5 to 50 h. The spectrum of pristine $Ca(BH_4)_2$ is shown as a reference. The dashed lines represent the ^{11}B CP-MAS NMR spectra and the small resonance at 0 ppm in pristine $Ca(BH_4)_2$ is owing to B-O impurities. [21]

Results

I. Hydrogen release at 350 °C

In the first series, $Ca(BH_4)_2$ was dehydrogenated under dynamic vacuum for 0.5 to 50 h at 350 °C, fairly below T_m. The ^{11}B MAS NMR spectra of the dehydrogenation products are shown in Fig. 1, together with the data of the $Ca(BH_4)_2$ starting material. The pristine sample showed two resonances at −30.1 ppm assigned to α-$Ca(BH_4)_2$ and at −32.7 ppm assigned to β-$Ca(BH_4)_2$.[21] After dehydrogenation at 350 °C for 0.5 h to 6 h, $Ca(BH_4)_2$ partially decomposed and two new resonances were observed at −14 ppm assigned to the formation of the CaB_2H_6 intermediate and at 11 ppm assigned to newly formed CaB_6. With increasing dehydrogenation time, the resonances attributed to the initial compound and the intermediate CaB_2H_6 disappeared and only the broad resonance of CaB_6 remained. The ^{1}H-^{11}B CP-MAS NMR spectra of samples recorded after 20 and 50 h of hydrogen release showed the absence of B-H bonds, indicating that $Ca(BH_4)_2$ fully decomposed and CaB_6 remained as the major product.

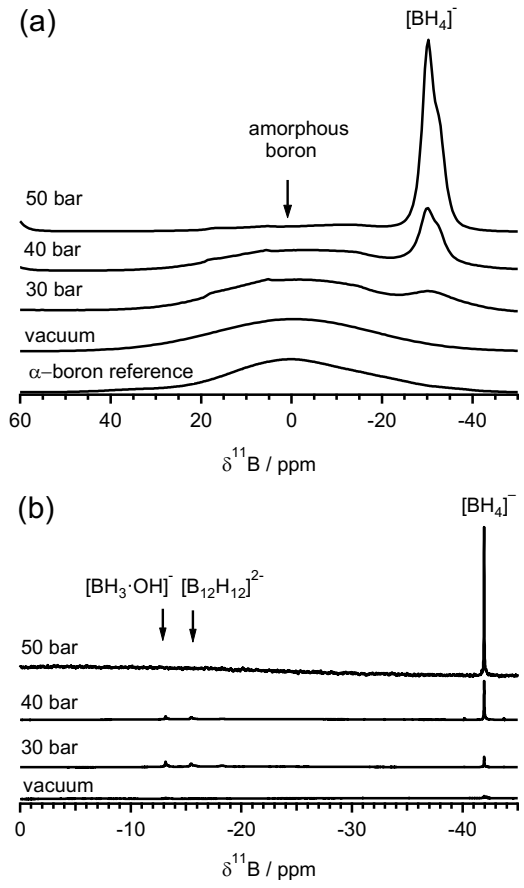

Fig. 2 (a) Solid-state ^{11}B MAS NMR spectra (α-boron shown as reference) and (b) solution-state ^{11}B NMR spectra recorded in aqueous solutions (pH = 14) of $Ca(BH_4)_2$ dehydrogenated at 400 °C under different H_2 backpressures from 50 bar to vacuum for 0.5 h.

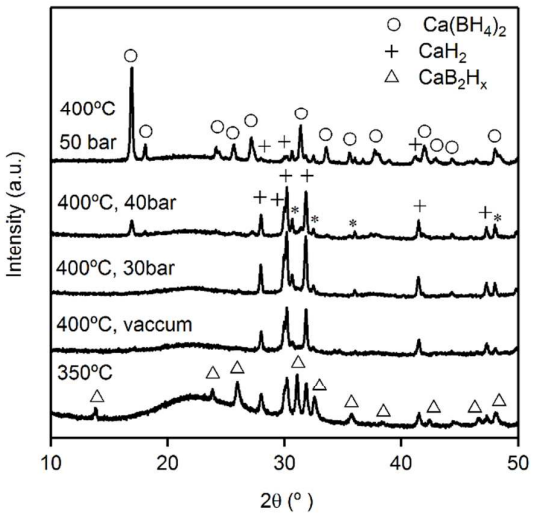

Fig. 3 XRD pattern of $Ca(BH_4)_2$ dehydrogenated at 400 °C under different H_2 backpressures for 0.5 h, compared to a dehydrogenation product obtained at 350°C for 2h. The asterisks represent some unidentified reflections, which are probably from contaminants.

II Hydrogen release at 400 °C

In order to study the dehydrogenation process of $Ca(BH_4)_2$ at temperatures above T_m (i.e. 400 °C), the decomposition of $Ca(BH_4)_2$ in the heating process was first suppressed by applying 200 bar of H_2. Subsequently, the H_2 pressure was stepwise reduced from 50 to 0 bar, respectively, which allowed the study of dehydrogenation at different H_2 backpressures. In the second series, we decomposed $Ca(BH_4)_2$ at 400°C within a fixed period of time of 0.5 h at various hydrogen backpressures. The ^{11}B MAS NMR spectra of the dehydrogenation products are shown in Fig. 2a. When $Ca(BH_4)_2$ was dehydrogenated at 50 bar H_2, a broad resonance centered at ca. 0 ppm assigned to amorphous boron was detected. Under a lower backpressure of 40 bar H_2, $Ca(BH_4)_2$ partially decomposed and the resonance assigned to amorphous boron significantly increased in the ^{11}B MAS NMR spectrum. Under a backpressure of 30 bar H_2, the resonance of $Ca(BH_4)_2$ further decreased and more amorphous boron was formed. Without H_2 backpressure, i.e. under dynamic vacuum, the decomposition of $Ca(BH_4)_2$ to amorphous boron was completed within 0.5 h. The ^{11}B NMR signals of CaB_6 or CaB_2H_6 phases were not observed in the decomposition products at 400 °C regardless of the applied H_2 backpressure.

The dehydrogenation products formed at 400 °C were leached in D_2O (pH=14) and investigated by solution state ^{11}B NMR (Fig. 2b) to track possible water-soluble intermediate phases in the solid residue, e.g., CaB_2H_6 or $CaB_{12}H_{12}$.[18] The resonance at –42 ppm assigned to $[BH_4]^-$ was observed in the dehydrogenation experiments performed at 50 to 30 bar H_2. The intensity of these resonances decreased significantly with decreasing H_2 backpressure, in line with the observation by solid-state ^{11}B MAS NMR results (Fig. 2a). No B-H intermediate phase was observed for the experiments with H_2 backpressure of 50 and 0 bar, respectively. Only traces of resonance at –13.1 ppm, assigned to $[BH_3{\cdot}OH]^-$,[18] and resonance at –15.2 ppm, assigned to $[B_{12}H_{12}]^{2-}$, were observed for the H_2 backpressure of 40 and 30 bar.

To corroborate the NMR data, XRD measurements of the decomposition products were carried out. The XRD pattern of the dehydrogenation products of $Ca(BH_4)_2$ obtained at 400 °C under different H_2 backpressures are shown in Fig. 3. Apparently, lower H_2 external pressure facilitated the dehydrogenation of $Ca(BH_4)_2$, and CaH_2 was identified as a dehydrogenation product. However, no intermediates such as CaB_2H_x were identified. In contrast, CaB_2H_x was observed as an intermediate when the dehydrogenation occurred at 350 °C. The XRD measurement results well fit the ^{11}B MAS NMR data (Figs. 1 and 2).

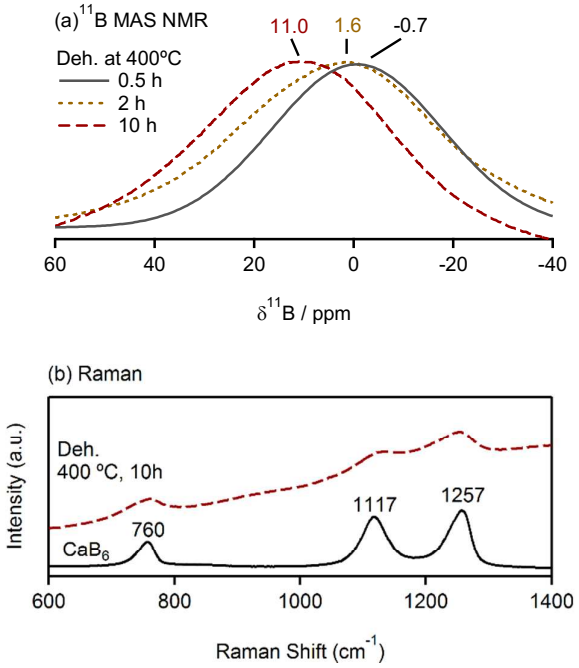

Fig. 4 (a) ^{11}B MAS NMR spectra of $Ca(BH_4)_2$ samples dehydrogenated at 400°C under vacuum for 0.5 to 10 h. (b) Raman spectrum of $Ca(BH_4)_2$ (400°C under vacuum for 10 h), compared to CaB_6 reference.

III Transformation of elemental boron to CaB_6

Motivated by the observation that amorphous boron was formed as a main decomposition product of $Ca(BH_4)_2$ at 400 °C, we continued the dehydrogenation process in a third series of samples. We further annealed the decomposition product from the second sample series, i.e. the one prepared at 400°C, under vacuum for 0.5 h. This sample showed a ^{11}B NMR chemical shift of –0.7 ppm, as displayed in Figure 4a. After annealing at 400 °C, the ^{11}B NMR chemical shift of the dehydrogenation products shifted from –0.7 ppm to 1.6 ppm after 2h and further to 11.0 ppm indicative for the possible formation of CaB_6. Longer annealing times did not further shift the resonance. The formation of CaB_6 was finally confirmed by Raman spectroscopy, as shown in Fig. 4b. The typical B-B modes of CaB_6 were observed at 760, 1117 and 1257 cm^{-1} in the spectrum of the annealed sample Thus, 10h sample treatment at 400 °C was

effective to convert elemental boron to CaB_6, a reaction paths which will benefit the rehydrogenation of $Ca(BH_4)_2$.

Discussion

In this study, we demonstrated two different routes to thermally decompose $Ca(BH_4)_2$ into CaB_6 and CaH_2 along two distinct reaction routes, as shown in Fig. 5. **Route 1**: Below T_m (e.g. at 350 °C) $Ca(BH_4)_2$ decomposes *via* CaB_2H_6 into CaB_6 and CaH_2 within 20 to 50 h under dynamic vacuum. **Route 2**: Above T_m (e.g. 400 °C) $Ca(BH_4)_2$ first decomposes *via* elemental boron and CaH_2, which converts to CaB_6 after further annealing under vacuum according to Eq. 5.

$$CaH_2 + 6B \rightarrow CaB_6 + H_2 \qquad (\Delta H = -50 \pm 19 \text{ kJ mol}^{-1} H_2) \quad (5)$$

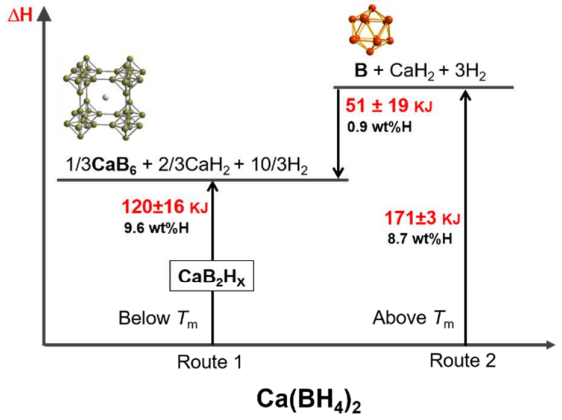

Fig. 5 Dehydrogenation routes with reaction enthalpies of $Ca(BH_4)_2$.

Obviously, the decomposition of $Ca(BH_4)_2$ into CaB_6 and CaH_2 is energetically more favorable than the reaction route resulting in the formation of elemental boron and CaH_2. Therefore, from a thermodynamic point of view the reason why the hydrogen release at 400 °C follows **Route 2** cannot be explained. However, there is a kinetic argument as schematically shown in Scheme 1: (1) When $Ca(BH_4)_2$ decomposes in the solid state (e.g. at 350 °C) and in dynamic vacuum, both routes are thermodynamically allowed. In addition, the conversion from $Ca(BH_4)_2$ to CaB_2H_x could maintain the sub-lattice of CaB_2 and thus probably avoid migration of Ca and B atoms in the solid. In contrast, dissociation from $Ca(BH_4)_2$ to CaH_2 and to B unavoidably involves the long-distance migration of Ca and B atoms resulting in a high energy barrier. (2) In liquid state the crystalline structure collapses and the ions can freely move. In this case the formation of CaH_2 and elemental boron is not hindered by steric arguments. Here, each Ca takes two H forming CaH_2, leaving B_2H_6 which immediately decomposes owing to its low thermal stability.[25] The further annealing of CaH_2 and elemental boron at 400 °C under vacuum finally leads to the formation of CaB_6, which is driven by the enthalpy change, i.e. about -50 ± 19 kJ mol^{-1} H_2.[5-7]

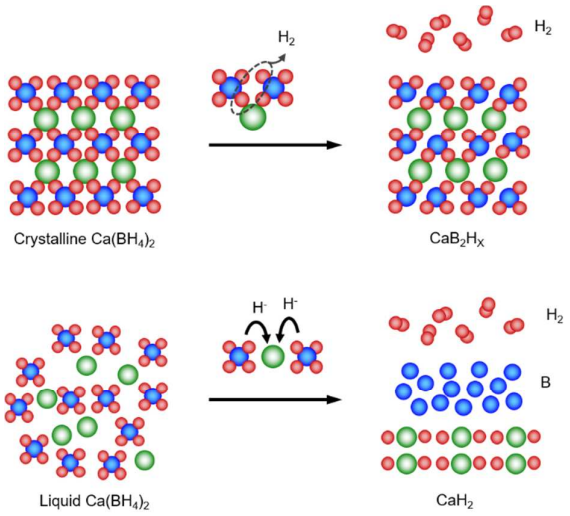

Scheme 1. Decomposition of $Ca(BH_4)_2$ in solid and liquid states.

Finally, we would like to discuss the role of $CaB_{12}H_{12}$ in the decomposition of $Ca(BH_4)_2$. The high stability of $CaB_{12}H_{12}$ has been reported and its decomposition into elemental boron requires temperatures above 750 °C.[26] The claim that $CaB_{12}H_{12}$ is an intermediate formed in the decomposition process of $Ca(BH_4)_2$ is based on the observation of a resonance between –10 to –20 ppm in solid state ^{11}B NMR spectra, i.e. very close to the ^{11}B NMR chemical shift of $CaB_{12}H_{12}$.[11-13] Recently, we identified this resonance to be assignable to CaB_2H_x (x = 6), supported by solution state ^{11}B NMR data and DFT calculations.[18] In the present study, only traces of $CaB_{12}H_{12}$ were observed when $Ca(BH_4)_2$ was dehydrogenated under H_2 backpressure at 400 °C, and no $CaB_{12}H_{12}$ was observed when the reaction was carried out under vacuum (Fig. 2b). The interpretation of our NMR data was confirmed by X-ray Raman scattering spectroscopy.[27] He et al. suggest that it is the presence of CaH_2 that favors the formation of CaB_6 over $CaB_{12}H_{12}$ in the decomposition of $Ca(BH_4)_2$.[26] Indeed, the reaction of CaH_2 and $CaB_{12}H_{12}$ to CaB_6 releases seven mol H_2 per mol $CaB_{12}H_{12}$, resulting in a huge entropy gain. Our observation that no $CaB_{12}H_{12}$ formed in dynamic vacuum, destabilizing the hydrides CaH_2 and $CaB_{12}H_{12}$, supports this argument.

Conclusion

We report two experimental protocols regarding the dehydrogenation of $Ca(BH_4)_2$ to CaB_6 and CaH_2.

Route 1: Below T_m at 350 °C, $Ca(BH_4)_2$ decomposes in the solid state *via* CaB_2H_6 into CaB_6 and CaH_2 under dynamic vacuum.

Route 2: Above T_m at 400 °C, $Ca(BH_4)_2$ decomposes into elemental boron and CaH_2, which further converts to CaB_6 after further annealing under vacuum.

The two routes are probably kinetically selected by the physical state of $Ca(BH_4)_2$ (solid or liquid) determining the initial decomposition step.

Only traces of $CaB_{12}H_{12}$ are detected as a byproduct of **Route 2** when H_2 backpressures of 30 to 50 bar are applied. Therefore, we believe that $Ca(BH_4)_2$ has a high potential to be used as a reversible hydrogen storage material.

Acknowledgements

We are grateful to The Innovation Fund Denmark (HyFill-Fast). The NMR hardware was partially granted by the Swiss National Science Foundation (SNFS, grant no. 206021_150638/1).

Notes and references

1. P. Jena, *The Journal of Physical Chemistry Letters*, 2011, **2**, 206-211.
2. M. B. Ley, L. H. Jepsen, Y.-S. Lee, Y. W. Cho, J. M. Bellosta von Colbe, M. Dornheim, M. Rokni, J. O. Jensen, M. Sloth, Y. Filinchuk, J. E. Jørgensen, F. Besenbacher and T. R. Jensen, *Mater Today*, 2014, **17**, 122-128.
3. H. W. Li, Y. G. Yan, S. Orimo, A. Zuttel and C. M. Jensen, *Energies*, 2011, **4**, 185-214.
4. Y. Liu, Y. Yang, M. Gao and H. Pan, *The Chemical Record*, 2016, **16**, 189-204.
5. K. Miwa, M. Aoki, T. Noritake, N. Ohba, Y. Nakamori, S. Towata, A. Zuttel and S. Orimo, *Phys Rev B*, 2006, **74**.
6. Y. Kim, D. Reed, Y. S. Lee, J. Y. Lee, J. H. Shim, D. Book and Y. W. Cho, *J Phys Chem C*, 2009, **113**, 5865-5871.
7. V. Ozolins, E. H. Majzoub and C. Wolverton, *J Am Chem Soc*, 2009, **131**, 230-237.
8. J.-H. Kim, S.-A. Jin, J.-H. Shim and Y. W. Cho, *J Alloy Compd*, 2008, **461**, L20-L22.
9. M. D. Riktor, M. H. Sorby, K. Chlopek, M. Fichtner and B. C. Hauback, *J Mater Chem*, 2009, **19**, 2754-2759.
10. L. L. Wang, D. D. Graham, I. M. Robertson and D. D. Johnson, *J Phys Chem C*, 2009, **113**, 20088-20096.
11. C. B. Minella, S. Garroni, D. Olid, F. Teixidor, C. Pistidda, I. Lindemann, O. Gutfleisch, M. D. Baro, R. Bormann, T. Klassen and M. Dornheim, *J Phys Chem C*, 2011, **115**, 18010-18014.
12. C. B. Minella, S. Garroni, C. Pistidda, R. Gosalawit-Utke, G. Barkhordarian, C. Rongeat, I. Lindemann, O. Gutfleisch, T. R. Jensen, Y. Cerenius, J. Christensen, M. D. Baro, R. Bormann, T. Klassen and M. Dornheim, *J Phys Chem C*, 2011, **115**, 2497-2504.
13. Y. Kim, S. J. Hwang, J. H. Shim, Y. S. Lee, H. N. Han and Y. W. Cho, *J Phys Chem C*, 2012, **116**, 4330-4334.
14. Y. Kim, S. J. Hwang, Y. S. Lee, J. Y. Suh, H. N. Han and Y. W. Cho, *J Phys Chem C*, 2012, **116**, 25715-25720.
15. H.-W. Li, E. Akiba and S.-i. Orimo, *J Alloy Compd*, 2013, **580, Supplement 1**, S292-S295.
16. J. Gu, M. X. Gao, H. G. Pan, Y. F. Liu, B. Li, Y. J. Yang, C. Liang, H. L. Fu and Z. X. Guo, *Energ Environ Sci*, 2013, **6**, 847-858.
17. M. D. Riktor, M. H. Sorby, J. Muller, E. G. Bardaji, M. Fichtner and B. C. Hauback, *J Alloy Compd*, 2015, **632**, 800-804.
18. Y. Yan, A. Remhof, D. Rentsch, A. Zuttel, S. Giri and P. Jena, *Chem Commun*, 2015, **51**, 11008-11011.
19. J. Huang, M. Gao, Z. Li, X. Cheng, J. Gu, Y. Liu and H. Pan, *J Alloy Compd*, 2016, **670**, 135-143.
20. N. Bergemann, C. Pistidda, C. Milanese, T. Emmler, F. Karimi, A. L. Chaudhary, M. R. Chierotti, T. Klassen and M. Dornheim, *Chem Commun*, 2016, **52**, 4836-4839.
21. Y. G. Yan, A. Remhof, P. Mauron, D. Rentsch, Z. Lodziana, Y. S. Lee, H. S. Lee, Y. W. Cho and A. Zuttel, *J Phys Chem C*, 2013, **117**, 8878-8886.
22. J. H. Shim, J. H. Lim, S. U. Rather, Y. S. Lee, D. Reed, Y. Kim, D. Book and Y. W. Cho, *J Phys Chem Lett*, 2010, **1**, 59-63.
23. Y. G. Yan, H. W. Li, H. Maekawa, K. Miwa, S. Towata and S. Orimo, *J Phys Chem C*, 2011, **115**, 19419-19423.
24. U. Bösenberg, S. Doppiu, L. Mosegaard, G. Barkhordarian, N. Eigen, A. Borgschulte, T. R. Jensen, Y. Cerenius, O. Gutfleisch, T. Klassen, M. Dornheim and R. Bormann, *Acta Mater*, 2007, **55**, 3951-3958.
25. O. Friedrichs, A. Remhof, A. Borgschulte, F. Buchter, S. I. Orimo and A. Zuttel, *Phys Chem Chem Phys*, 2010, **12**, 10919-10922.
26. L. He, H.-W. Li, N. Tumanov, Y. Filinchuk and E. Akiba, *Dalton T*, 2015, **44**, 15882-15887.
27. C. J. Sahle, C. Sternemann, C. Giacobbe, Y. Yan, C. Weis, M. Harder, Y. Forov, G. Spiekermann, M. Tolan, M. Krisch and A. Remhof, *Phys Chem Chem Phys*, 2016, **18**, 19866-19872.